Available online at www.sciencedirect.com
ScienceDirect
Molecular Phylogenetics and Evolution 42 (2007) 637–652
MOLECULAR PHYLOGENETICS AND EVOLUTION
www.elsevier.com/locate/ympev

Phylogenetics of the woodrat genus *Neotoma* (Rodentia: Muridae): Implications for the evolution of phenotypic variation in male external genitalia

Marjorie D. Matocq [a,*], Quinn R. Shurtliff [a], Chris R. Feldman [b]

[a] *Department of Biological Sciences, Idaho State University, Campus Box 8007, Pocatello, ID 83209, USA*
[b] *Department of Biology, Utah State University, Logan UT, 84322-5305, USA*

Received 21 October 2005; accepted 15 August 2006
Available online 15 November 2006

Abstract

Interspecific morphological variation in animal genitalia has long attracted the attention of evolutionary biologists because of the role genital form may play in the generation and/or maintenance of species boundaries. Here we examine the origin and evolution of genital variation in rodents of the muroid genus *Neotoma*. We test the hypothesis that a relatively rare genital form has evolved only once in *Neotoma*. We use four mitochondrial and four nuclear markers to evaluate this hypothesis by establishing a phylogenetic framework in which to examine genital evolution. We find intron seven of the β-fibrinogen gene to be a highly informative nuclear marker for the levels of differentiation that characterize *Neotoma* with this locus evolving at a rate slower than cytochrome *b* but faster than 12S. We estimate phylogenetic relationships within *Neotoma* using both maximum parsimony and maximum likelihood-based Bayesian methods. Our Bayesian and parsimony reconstructions differ in significant ways, but we show that our parsimony analysis may be influenced by long-branch attraction. Furthermore, our estimate of *Neotoma* phylogeny remains consistent across various data partitioning strategies in the Bayesian analyses. Using ancestral state reconstruction, we find support for the monophyly of taxa that possess the relatively rare genital form. However, we also find support for the independent evolution of the common genital form and discuss possible underlying developmental shifts that may have contributed to our observed patterns of morphological evolution.

Keywords: *Neotoma*; Phylogeny; Ancestral state reconstruction; Genital evolution; β-Fibrinogen

1. Introduction

Divergence of reproduction-associated traits among species has been documented at the phenotypic and molecular level for several systems including gamete recognition (Vacquier et al., 1997), spermatogenesis (Wyckoff et al., 2000), and pheromones (Sanchez-Gracia et al., 2003; Watts et al., 2004). Divergence in these systems is of particular interest to evolutionary biologists because of the role these systems play in reproductive compatibility/isolation and thus, potentially, the process of speciation. Another highly variable reproduction-associated system is that of external genitalia. Many animal groups are characterized by striking levels of phenotypic variation in male external genitalia, even among closely related species that are otherwise undifferentiated (Hooper, 1960; Eberhard, 1985; Arnqvist, 1997). In mammals, interspecific variation in external genitalia is pronounced in many groups (Krutzch and Vaughn, 1955; Hooper, 1960; Prasad, 1974; Hershkovitz, 1979; Short, 1979; Martin and Schmidly, 1982), has long been used as an important taxonomic character (Hooper, 1958; Hooper and Musser, 1964; Lidicker, 1968; Lidicker and Brylski, 1987; Bradley and Schmidly, 1987; Sullivan et al., 1990), and likely contributes to reproductive isolation between species (Long and Frank, 1968; Patterson and Thaeler, 1982). Data from laboratory rats and other

* Corresponding author. Fax: +1 208 282 4570.
E-mail addresses: matomarj@isu.edu (M.D. Matocq), shurquin@isu.edu (Q.R. Shurtliff), elgaria@biology.usu.edu (C.R. Feldman).

1055-7903/$ - see front matter © 2006 Elsevier Inc. All rights reserved.
doi:10.1016/j.ympev.2006.08.011

muroid rodents suggest that male genital morphology and copulatory behavior impact rates of fertilization and breeding success (Adler, 1969; Dewsbury, 1975; Matthews and Adler, 1977). As such, the link between phenotypic variation in external genitalia and the establishment and/or maintenance of reproductive barriers, and thus speciation, in mammals seems plausible and yet remains poorly understood (Patterson and Thaeler, 1982).

One group of muroid rodents that is characterized by particularly trenchant morphological differences in male external genitalia is the woodrat genus *Neotoma* (Muridae). Variation in male external genitalia (referred to as the phallus or glans penis) ranges from "oblong", or relatively broad forms, to partially and completely narrow forms (Hooper, 1960; Matocq, 2002a) (Fig. 1). The broad-form phallus is correlated with copulatory locking behavior in *Neotoma* and other rodents whereas species with narrow phalli have not been observed to exhibit such behavior (Dewsbury, 1975). Thus, there are significant behavioral and functional differences among species with these different phallus morphologies.

Although Hooper's original work on *Neotoma* (1960) did not discuss the evolution of phallus morphology in modern phylogenetic terms, he did suggest that, although unique from one another, the partially and completely narrow forms were separate from the group of broad-form taxa. Furthermore, he suggested a morphological gradation from the broad form, to a partially narrow form, to the completely narrow form (Fig. 1). This would imply the monophyly (single evolution) of narrow forms. However, the most recent phylogenetic study of the genus *Neotoma* based on cytochrome *b* sequence analysis (Edwards and Bradley, 2002) suggested a distant relationship between some narrow-formed taxa implying this morphology has arisen more than once in the history of the taxon.

In order to gain insight into the evolution of phenotypic variation in male external genitalia in the genus *Neotoma,* we reconstruct phylogenetic relationships within the group using four mitochondrial and four nuclear loci. We assess the phylogenetic utility of the nuclear loci by comparison to more commonly used mitochondrial markers. We also use various ancestral state reconstruction methods to estimate the number of gains/losses of particular genital morphological states in the genus. Specifically, we test Hooper's hypothesis of a monophyletic, narrow-phallus clade versus a multiple origins hypothesis. Based on our inferred patterns of morphological evolution, we suggest how developmental trajectories may have evolved to produce these patterns. Our study provides insight into the evolutionary lability of genital morphology in this group and identifies clades that exhibit particularly high levels of variation in this reproduction-associated character.

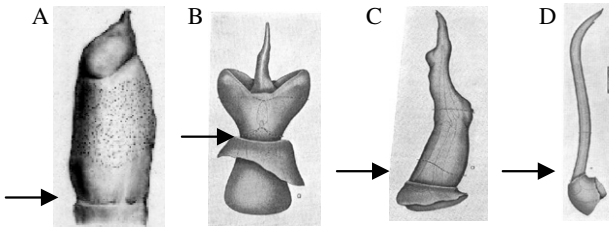

Fig. 1. Morphological variation in the male external genitalia of four members of the genus *Neotoma*. (A) *N. fuscipes*, (B) *N. macrotis*, (C) *N. cinerea*, (D) *N. lepida*. Arrows point to the base of the glans penis where the prepuce attaches. Prepuce is pulled back and cut away. Specimens are not shown to scale. Illustration A by Karen Klitz and B, C, and D reproduced from Hooper (1960) with permission from the University of Michigan Museum of Zoology.

2. Materials and methods

2.1. Taxon sampling

We collected DNA sequence data from 47 specimens (including *Xenomys nelsoni* and *Hodomys alleni*) representing 14 *Neotoma* species from each of the well-supported species groups recognized by Edwards and Bradley (2002), as well as newly identified subdivisions within the *Neotoma fuscipes* (Matocq, 2002a,b) and *Neotoma lepida* (Patton and Álvarez-Castañeda, 2005) complexes (Appendix A). To polarize the characters, we used progressively distantly related taxa including *Peromyscus attwateri*, *Tylomys nudicaudus*, and *Ototylomys phyllotis*, following Edwards and Bradley (2002) and Reeder and Bradley (2004). We used the same vouchered specimens as Edwards and Bradley (2002) to represent the majority of the species groups (Appendix A).

2.2. Genomic sampling

Because different portions of the nuclear and mitochondrial genomes evolve at vastly different rates, we can target specific regions of those genomes to provide resolution at various phylogenetic levels. The previous molecular systematic treatment of *Neotoma* (Edwards and Bradley, 2002) used cytochrome *b* sequences, a rapidly evolving mtDNA locus widely used to resolve intra- and interspecific relationships in rodents (Bradley and Baker, 2001; Matocq, 2002b; Lessa et al., 2003). Accordingly, Edwards and Bradley (2002) found cytochrome *b* useful in identifying the major species assemblages within *Neotoma*, but poor at resolving relationships among these groups. As such, we sampled eight markers in an effort to encompass a broad range of evolutionary rates, from rapidly evolving mitochondrial regions to nuclear exons. We chose four mitochondrial regions that include portions of the small subunit rRNA (12S; 531bp), large subunit rRNA (16S; 571bp), cytochrome *c* oxidase subunit II (COII; 633bp), and the entire cytochrome *b* locus (cyt *b*; 1143bp). We also sampled four nuclear markers that consist of fragments of mineralocorticoid receptor exon 3 (MLR; 205bp), myosin heavy polypeptide 6 α exon 35 and intron 35 (MYH6; 236bp), engrailed 2 exon 3 (EN2; 146bp) and the entire intron 7 of β-fibrinogen (FGB; 777bp).

2.3. Laboratory protocols

We isolated and purified genomic DNA from liver tissue with the DNeasy Tissue Kit (Qiagen, Inc.). We amplified the eight markers (four mitochondrial and four nuclear) via PCR (Saiki et al., 1988) using the primers listed in Table 1. We used the following thermal cycle parameters for 25 μl amplification reactions: 1 cycle of 5–10 min denaturation at 94 °C; 33 cycles of 1 min denaturation at 94 °C, 1 min anneal at 45 °C (cyt *b*, 16S), 51 °C (COII), 56 °C (MLR), 57 °C (EN2), 60 °C (FGB), 62 °C (MYH6, 12S), and 1 min extension at 72 °C. We cleaned amplified products using the QIAquick PCR Purification Kit (Qiagen, Inc.) and used purified template in 10 μl dideoxy chain-termination reactions (Sanger et al., 1977) using ABI Big Dye chemistry (Applied Biosystems, Inc.) and the primers in Table 1. Following an isopropanol/ethanol precipitation, we ran cycle-sequenced products on an ABI 3100 automated sequencer (Applied Biosystems, Inc.) located in the Molecular Research Core Facility at Idaho State University (http://www.mrcf.isu.edu/). We sequenced all samples in both directions.

2.4. Sequence analyses

We aligned DNA sequences in the program Sequencher™ 4.1.2 (Gene Codes Corp.), verified alignments by eye, and translated protein coding nucleotide sequences into amino acid sequences using MacClade 4.0 (Maddison and Maddison, 2005). We deposited all DNA sequences in GenBank (Appendix A).

We assessed rates of evolution in the four nuclear markers through comparison to two widely used mitochondrial markers, 12S and cyt *b*. We chose 12S and cyt *b* as benchmark "slow" and "fast" mtDNA loci, respectively. To compare rate differences between the nuclear markers and 12S and cyt *b*, we first computed uncorrected pairwise sequence differences between terminal taxa in PAUP* 4.0b10 (Swofford, 2002) for each marker. We then plotted the *p*-distances of 12S and cyt *b* versus the *p*-distance of the nuclear fragments. Finally, we employed a one-sample *t*-test (p. 328, Grafen and Hails, 2004) to determine whether the regression of each nuclear marker versus 12S and cyt *b* deviated significantly from a slope of one (i.e., evolves at a rate significantly different than 12S or cyt *b*). This approach should be less sensitive and more accurate than applying a χ^2 or Wilcoxon signed-ranks test because it includes information on the magnitude of difference between two markers for each comparison (Feldman and Omland, 2005).

2.5. Phylogenetic analyses

We used maximum parsimony (MP; Farris, 1983) and Bayesian inference (BI; Larget and Simon, 1999) phylogenetic methods on the combined data of all markers to establish evolutionary relationships of *Neotoma* lineages. We conducted MP phylogenetic analyses in PAUP* and BI analyses with MrBayes 3.1.1 (Huelsenbeck and Ronquist, 2001;Ronquist and Huelsenbeck, 2003).

We executed MP analyses with the heuristic search algorithm using TBR branch swapping and 1000 random sequence additions. We weighted characters equally and

Table 1
Oligonucleotide primers used to amplify and sequence mtDNA and nucDNA in *Neotoma* and related taxa

Locus	Primer	Sequence	Source
cyt *b*[a]	MVZ05	5′-CGA AGC TTG ATA TGA AAA ACC ATC GTT G-3′	Irwin et al. (1991)
	MVZ16	5′-AAA TAG GAA RTA TCA YTC TGG TTT RAT-3′	Smith and Patton (1993)
	cytb2a	5′-CAG GAT CCA ACA ACC CAA CAG G-3′	This study
	MVZ14	5′-GGT CTT CAT CTY HGG YTT ACA AGA C-3′	Smith and Patton (1993)
COII	COIIa	5′-AAC CAT TTC ATA ACT TTG TCA A-3′	Adkins and Honeycutt (1994)
	COIIb	5′-CTC TTA ATC TTT AAC TTA AAA G-3′	Adkins and Honeycutt (1994)
12S	12Sa	5′-AAA CTG GGA TTA GAT ACC CCA C-3′	This study
	12Sb	5′-CAC TTT CCA GTA TGC TTA CCT TG-3′	This study
16S	16Sa	5′-CGC CTG TTT ACC AAA AAC AT-3′	This study
	16Sb	5′-GAT CAC GTA GGA CTT TAA TCG-3′	This study
EN2	EN2f	5′-CCC GAA AAC CAA AGA AGA AG-3′	Lyons et al. (1997)
	EN2r	5′-GTT CTG GAA CCA AAT CTT GAT C-3′	Lyons et al. (1997)
MLR	MLRf	5′-GCT CAG TTT CCA GCC CTT C-3′	Lyons et al. (1997)
	MLRr	5′-AGT CAC ACC ATT TGA GAT GGC-3′	Lyons et al. (1997)
MYH6[b]	MYH2f	5′-GAA CAC CAG CCT CAT CAA CC-3′	Lyons et al. (1997)
	MHY2r	5′-TGG TGT CCT GCT CCT TCT TC-3′	Lyons et al. (1997)
FGB	β17-mammL	5′-ACC CCA GTA GTA TCT GCC GTT TGG ATT-3′	This study
	βfib-mammU	5′-CAC AAC GGC ATG TTC TTC AGC AC-3′	This study

[a] Ambiguity code: H, not G; R, A or G; Y, C or T.
[b] The primers we report here for MYH6 were originally designed for MYH2 (Lyons et al., 1997). However, a nucleotide-nucleotide BLAST search (Altschul et al., 1997) in GenBank indicates that the fragment we sequenced is MYH6.

coded gaps as fifth character states because most indels occurred as single base pair substitutions. However, several large indels occurred in FGB that we treated as a single character (deletion 0, insertion 1) following Prychitko and Moore (2003) and Feldman and Omland (2005). We also coded multiple state positions in nuclear loci as polymorphic. To assess nodal support, we used the bootstrap resampling method (Felsenstein, 1985) employing 1000 pseudoreplicates of heuristic searches using TBR branch swapping and 100 random sequence additions in PAUP*. Additionally, we calculated branch support (Bremer, 1994) for all nodes using the program Tree Rot 2c (Sorenson, 1999).

We performed BI analyses to estimate branch lengths and search for additional tree topologies. Previous model-based approaches have been restricted to the use of a single model of DNA evolution across an entire dataset. If the dataset contains multiple loci that possess different functional constraints, biochemical properties, and patterns of evolution, then a single model of molecular evolution may simply represent a compromise among the different loci (reviewed in Brandley et al., 2005). Such an approach may be problematic if the single model of evolution inadequately describes patterns of nucleotide substitution in the dataset, leading to error that can mislead phylogenetic analyses (Yang, 1996; Swofford et al., 1996; Brandley et al., 2005). However, mixed-model phylogenetic analyses (Yang, 1996) may also be associated with greater topological uncertainty (Nylander et al., 2004; Brandley et al., 2005). Thus we performed three BI tree searches, one without data partitions (one model for all DNA; P_1), a second search with two data partitions (a model for mtDNA and nucDNA; P_2), and a final search with eight data partitions (a model for each locus; P_8). We follow the notation of Brandley et al. (2005), where P corresponds to a partition, and a numerical subscript denotes the number of data partitions. We evaluated the fit of various models of molecular evolution to our different data partitions (Table 3) with the Akaike Information Criterion (AIC; Akaike, 1974) in the program MrModeltest 2.1 (Nylander, 2004). The AIC has recently been shown to be a superior method of model selection in comparison to hierarchical likelihood ratio tests (Posada and Buckley, 2004). For each BI search we did not specify nucleotide substitution model parameters or a topology *a priori*. We ran BI analyses for 3×10^6 generations using the default temperature (0.2) with four Markov chains per generation, sampling trees every 100 generations. We then computed a 50% majority-rule consensus tree after excluding those trees sampled prior to the stable equilibrium, yielding estimates of nodal support (i.e., posterior probability of a clade) given by the frequency of the recovered clade (Rannala and Yang, 1996; Huelsenbeck and Ronquist, 2001).

2.6. Topology tests

We assessed the congruence between MP and BI hypotheses of *Neotoma* phylogeny using constraint searches and subsequent topology tests. First, we constrained the equally weighted MP searches to retain only those trees with the major topological difference recovered in the BI analyses (see Section 3). We then compared the constrained and unconstrained MP estimates of *Neotoma* phylogeny using a two-tailed Wilcoxon signed-ranks test (Templeton, 1983).

Similarly, we constrained the three BI searches to recover only those trees with the major topological difference found in the MP analysis. We then compared the $-\ln L$ values from the entire set of post-burnin constrained and unconstrained BI trees using a non-parametric Mann–Whitney *U*-test (Sokal and Rohlf, 1995). Additionally, we used the Bayes factor to compare the weight of evidence for the two competing hypotheses (Kass and Raftery, 1995). The Bayes factor is not a standard statistical test resulting in the acceptance or rejection of hypotheses based on critical values, but instead provides some information on the relative ability of two hypotheses to explain the data (Kass and Raftery, 1995). Because the Bayes factor can be used to compare models that are not hierarchically nested (Nylander et al., 2004), we employed it to evaluate the hypothesis that our constrained and unconstrained BI topologies explain the data equally well (H_0), versus the alternative that constraint BI searches provide a poorer explanation of the data (H_1). We calculated the Bayes factor as twice the difference in the harmonic mean $-\ln L$ scores ($2\ln B_{01}$) between alternative hypotheses (Brandley et al., 2005) and compared these values to the framework provided by Kass and Raftery (1995) where <0 is evidence against H_1, 0–2 provides no evidence for H_1, 2–6 is positive support for H_1, 6–10 is strong support for H_1, and >10 is very strong support for H_1 (see Nylander et al., 2004; Brandley et al., 2005).

2.7. Ancestral state reconstruction

To understand the evolution of phallus morphology in *Neotoma*, we reconstructed the pattern of character changes on our MP and BI phylogenetic hypotheses. All ancestral state reconstructions were conducted by tracing characters over trees in Mesquite 1.05 (Maddison and Maddison, 2004). We scored each OTU using descriptions from the literature (Hooper, 1960; Matocq, 2002a) and from examination of fluid preserved specimens (Appendix B) as possessing one of two character states: 0-broad/oblong phallus (Fig. 1A), 1-partially or completely narrow phallus (Fig. 1B–D). Taxa with narrow phallus morphotypes are *P. attwateri*, *N. lepida*, *N. cinerea*, and *N. macrotis*; all other taxa possess broad/oblong phalli. Although variation in phallic structure exists within the *N. lepida* complex (Mascarello, 1978; Patton and Álvarez-Castañeda, 2005), all variants are of the narrow form.

We used both MP and maximum likelihood (ML) methods of ancestral state reconstruction (Schluter et al., 1997; Pagel, 1999). Parsimony ancestral state reconstruction minimizes the amount of character change given a tree topology and character state distribution. Parsimony ancestral

state reconstruction has been widely used but may overrepresent confidence in ancestral character states (Schluter et al., 1997). A ML approach takes into account branch lengths and estimates probabilities of all possible character states at each node, thus providing an estimate of uncertainty in ancestral state reconstruction (Pagel, 1999). In addition to uncertainty in character reconstruction on a single tree, we took into account nodal uncertainty by making our estimates over sets of trees (Lutzoni et al., 2001). The MP set included all of the most parsimonious trees, while the ML set included the post-burnin samples of BI trees from the P_8 analysis. In MP ancestral state reconstruction, on both the MP and BI tree sets, we considered character transitions to be unordered (Fitch parsimony). One character or the other was assigned to a node if it created fewer steps, otherwise the node was considered equivocal. In ML ancestral state reconstruction, on both MP and BI tree sets, we used a Markov *k*-state one-parameter model (Mk-1; Lewis, 2001) that considers any change equally probable. Branch lengths were those generated in the original MP and BI searches. Zero length branches are not accepted in ML ancestral state reconstruction analyses, thus, we changed zero values to one (Hibbett and Donoghue, 2001). A state was assigned to a node if its probability exceeded a decision threshold of two (i.e., ~7.4 times more probable than the alternative state) otherwise, the node was considered equivocal.

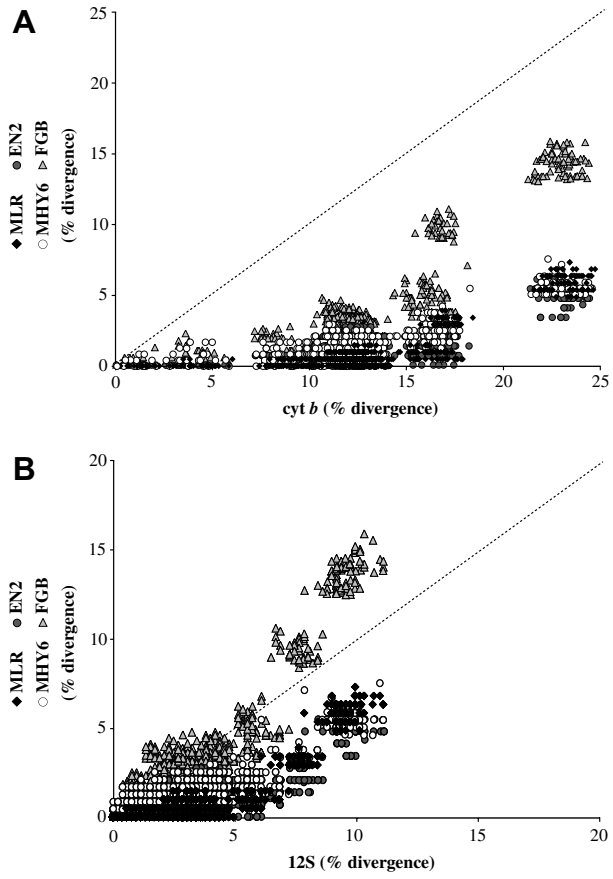

Fig. 2. Scatter diagrams of uncorrected pairwise sequence divergence for two benchmark mitochondrial loci versus the four nuclear markers. The dashed line corresponds to $x = y$, for which pairwise divergence values are equal for the mitochondrial and nuclear fragments being compared. (A) Each nuclear marker displays a significantly slower rate of evolution than our benchmark "fast" mtDNA locus, cyt *b* (MLR: $t = -233.1$, $P < 0.0001$; MYH6: $t = -430.7$, $P < 0.0001$; EN2: $t = -530.7$, $P < 0.0001$; FGB: $t = -29.5$, $P < 0.0001$). (B) Three of the four nuclear markers also show a distinctly slower rate of evolution than our "slow" mtDNA locus, 12S (MLR: $t = -58.6$, $P < 0.0001$; MYH6: $t = -77.4$, $P < 0.0001$; EN2: $t = -122.7$, $P < 0.0001$). However, the seventh intron of FGB appears to be evolving more rapidly than 12S ($t = 13.5$, $P < 0.0001$).

3. Results

3.1. Genetic variation

Sequences from the protein coding regions in both mitochondrial and nuclear fragments appear functional. Our final alignment contains 4040 nucleotides (2878bp mtDNA, 1162bp nucDNA) after the exclusion of 204bp of indels from FGB, yielding 994 parsimony informative sites (846 mtDNA, 148 nucDNA) (Table 2). Among mtDNA loci, cyt

Table 2
Summary statistics from MP analyses of the various data partitions

Partition	No. of characters	No. of informative characters	Proportion of informative characters (%)	Mean sequence divergence[a] (%)	No. of MP trees	MP tree score (L)	MP tree score (CI / RI)	No. of resolved nodes	Proportion of resolved nodes (%)
all DNA	4040	994	24.60	7.34	3	4631	0.42/0.68	46	97.87
mtDNA	2878	846	29.40	9.30	9	4121	0.37/0.69	45	95.74
nucDNA	1162	148	12.74	2.44	10,001	315	0.69/0.84	21	44.68
12S	531	86	16.20	3.79	709	279	0.56/0.76	29	61.70
16S	571	104	18.21	4.37	909	432	0.50/0.70	26	55.32
COII	633	211	33.33	11.39	24	1049	0.35/0.70	40	85.11
cytb	1143	445	38.93	12.89	6	2312	0.35/0.65	45	95.74
MLR	205	10	4.88	0.95	12	31	0.94/0.92	3	6.38
MYH6	238	15	6.30	1.42	1947	68	0.81/0.83	5	10.64
EN2	146	9	6.16	1.44	12	21	0.91/0.96	6	12.77
FGB	573	114	19.90	3.45	25,372	346	0.82/0.87	19	40.43

Note. Values include outgroup samples and gaps as fifth character states. Only FGB possesses gaps larger than a single nucleotide position, and we coded these indels as single characters (deletion 0, insertion 1).

[a] Uncorrected *p*-distance.

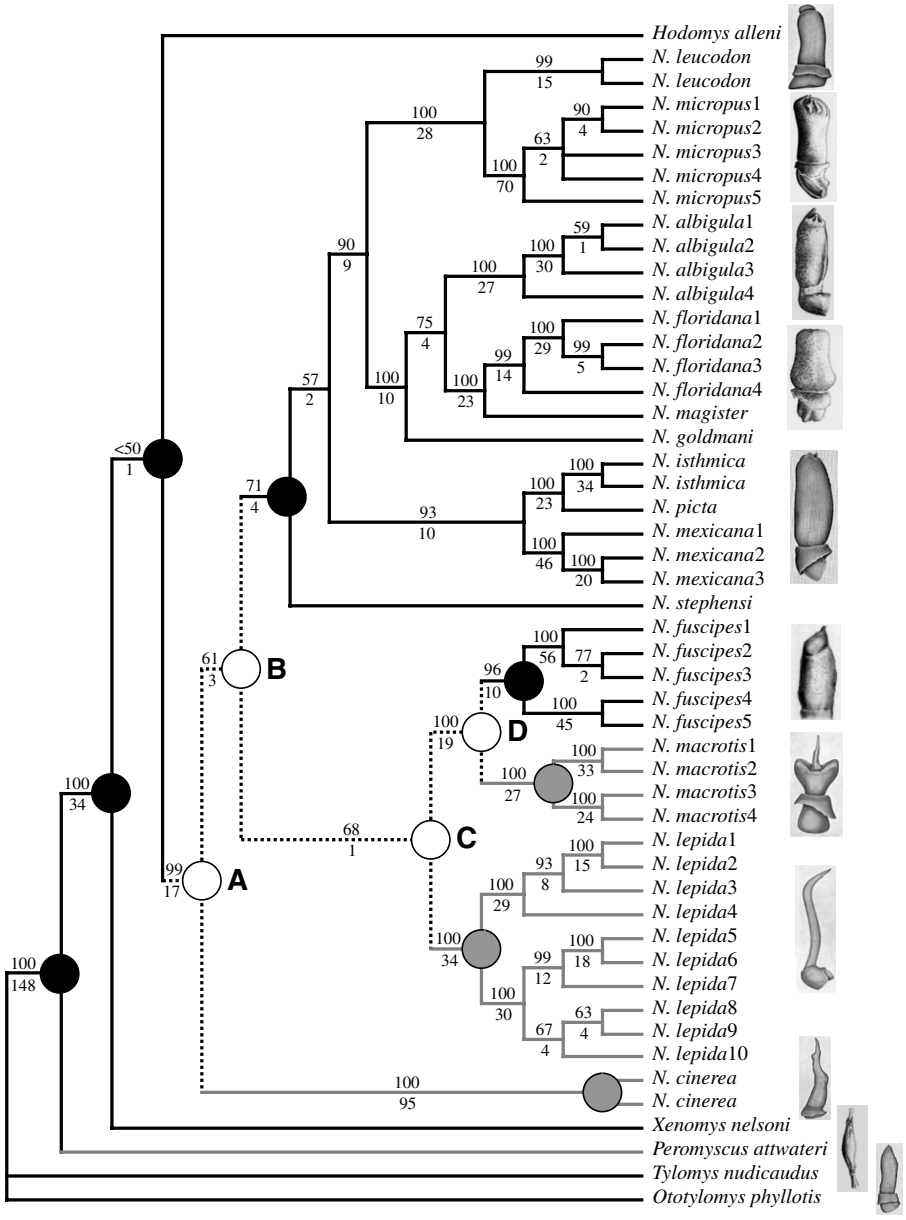

Fig. 3. Phylogenetic hypothesis of *Neotoma* relationships based on combined MP analysis of equally weighted mitochondrial and nuclear characters. The topology is a strict consensus of three equally optimal trees ($L = 4631$, CI = 0.42, RI = 0.68). Numbers above nodes indicate bootstrap support, while those below represent decay indices. Also shown is the MP reconstruction of phallus evolution in *Neotoma*. Lineages reconstructed with broad phalli illustrated with black lines (nodes with black circles), those with partially and completely narrow phalli with grey lines (nodes with grey circles), and those of uncertain ancestral state with dashed lines (nodes with white circles). Lettered nodes refer to discussion of character evolution in text. Specimens are not shown to scale. Illustrations by Karen Klitz, Q. R.S. and reproduced from Hooper (1960) with permission from the University of Michigan Museum of Zoology.

b possesses both the largest number and highest proportion of informative sites (445, 38.9%), as does FGB among nuclear fragments (114, 19.9%) (Table 2). All of the nuclear markers display a significantly slower rate of evolution than our benchmark "fast" mitochondrial locus, cyt *b* (MLR: $t = -233.1$, $P < 0.0001$; MYH6: $t = -430.7$, $P < 0.0001$; EN2: $t = -530.7$, $P < 0.0001$; FGB: $t = -29.5$, $P < 0.0001$) (Fig. 2). Additionally, three nuclear markers also show a noticeably slower rate of evolution than our "slow" mitochondrial locus, 12S (MLR: $t = -58.6$, $P < 0.0001$; MYH6: $t = -77.4$, $P < 0.0001$; EN2: $t = -122.7$, $P < 0.0001$) (Fig. 2). However, rate comparisons between FGB and 12S suggest that FGB is evolving more rapidly than12S ($t = 13.5$, $P < 0.0001$) (Fig. 2).

We did note some discrepancies between the cyt *b* sequences generated here and those in Edwards and Bradley (2002), despite the fact that the same source material was used (Appendix A). Some of the discrepancies are due to GenBank uploading errors associated with the previous study (Bradley, R.D. personal communication) but others are genuine sequence differences. Even with the largest discrepancies between the studies, sequences from the same individual are still most similar to each other in comparison to all other *Neotoma* sequences available. As such,

Table 3
Parameter estimates from the three separate BI analyses using different data partitions

Partition type Partition	Model of DNA substitution[a]	Mean α	Mean P_{inv}	Mean ti/tv	Mean πA	Mean πC	Mean πG	Mean πT	Mean rA–C	Mean rA–G	Mean rA–T	Mean rC–G	Mean rC–T	Mean rG–T
P_1														
all DNA	GTR + I + Γ	0.6425	0.5662	—	0.3268	0.2822	0.1581	0.2328	1.5144	7.4388	1.6643	0.3448	24.0204	1
P_2														
mtDNA	GTR + I + Γ	0.9737	0.5983	—	0.3549	0.2922	0.1191	0.2339	2.9027	21.9038	3.4885	0.5503	52.3111	1
nucDNA	GTR + I + Γ	0.1977	0.4943	—	0.2774	0.2562	0.2368	0.2296	0.6563	3.1893	0.4536	0.4039	3.3711	1
P_8														
12S	GTR + I + Γ	0.3700	0.5997	—	0.3690	0.2110	0.1625	0.2575	0.9987	4.2578	1.1733	0.2993	28.0132	1
16S	GTR + I + Γ	0.5123	0.6380	—	0.3329	0.2125	0.1761	0.2785	9.8016	17.5304	9.2750	0.7621	124.9231	1
COII	GTR + I + Γ	1.7798	0.5967	—	0.3704	0.2901	0.0940	0.2456	0.9737	18.9796	1.9454	0.1968	30.0450	1
cyt *b*	GTR + I + Γ	0.9667	0.5509	—	0.3568	0.3485	0.0759	0.2187	2.3902	33.1296	2.3925	1.5512	40.0907	1
MLR	HKY + Γ	0.1046	—	5.1368	0.2413	0.3360	0.2447	0.1780	—	—	—	—	—	—
MYH6	GTR + I + Γ	0.2161	0.6738	—	0.2437	0.3036	0.3148	0.1379	0.1034	1.0149	0.3784	0.1360	2.3617	1
EN2	HKY + Γ	0.1054	—	5.0577	0.2985	0.2893	0.2960	0.1163	—	—	—	—	—	—
FGB	GTR + Γ	0.1879	—	—	0.3050	0.2093	0.1919	0.2938	0.8871	4.1688	0.3604	0.8952	4.6152	1

Note. Parameter estimates represent mean values from the 29,000 sampled BI trees.
[a] Best fit model of DNA evolution estimated using AIC in MrModeltest 2.1.

differences in tree topologies between our study and Edwards and Bradley (2002) are not due to sequence discrepancies in cyt *b*.

3.2. Phylogenetic relationships

The equally weighted MP analysis yielded three optimal trees ($L = 4631$, CI = 0.42, RI = 0.68) (Table 2 and Fig. 3). The three BI analyses all reached stable parameter estimates within the first 100,000 generations (Table 3). Thus each 50% majority-rule consensus tree (P_1: harmonic mean $-\ln L = 26147.7036$; P_2: $-\ln L = 26011.3972$; P_8: $-\ln L = 25885.9923$) from three BI analyses is based on nearly 30,000 sampled trees. These three BI consensus trees show nearly identical topologies and support values to each other (Fig. 4), and are generally similar to the strict consensus MP tree.

In all analyses, *Xenomys nelsoni* and *Hodomys alleni* form a clade with *Neotoma* (bootstrap percent 100, decay index 34, posterior probability for all analyses 100) but the MP analysis weakly places *H. alleni* as sister to *Neotoma* (BP < 50, DI 1), while the BI analyses firmly connect *H. alleni* and *X. nelsoni* (PP 100). Both MP and BI strongly support the monophyly of *Neotoma* (BP 99, DI 17, PP 100) but differ in the placement of the deepest divergence within *Neotoma*. In the MP analysis the deepest split within *Neotoma* occurs between the bushy-tailed woodrat, *N. cinerea*, and a clade composed of all other woodrat taxa (BP 61, DI 3). The MP analysis further divides *Neotoma* into one of two major clades; a *N. fuscipes* + *N. macrotis* + *N. lepida* clade (BP 68, DI 1), and a second clade containing the remaining woodrat species (BP 71, DI 4). The BI analyses, on the other hand, place *N. cinerea* within the *N. fuscipes* + *N. macrotis* + *N. lepida* clade (PP 99–95) as the lineage sister to the clade of all other *Neotoma* taxa (PP 97–94). All analyses support the monophyly of the *N. lepida* complex (BP 100, DI 34, PP 100), *N. fuscipes* (BP 96, DI 10, PP 100), and *N. macrotis* (BP 100, DI 27, PP 100), as well as the connection of the latter two species (BP 100, DI 19, PP 100). However, the placement of *N. cinerea* is less certain. All three BI analyses connect *N. cinerea* to the *N. fuscipes* + *N. macrotis* clade, but at low frequencies (PP 84–56).

The second major woodrat clade is composed of three subclades: a clade containing *N. mexicana*, *N. isthmica*, and *N. picta* (BP 93, DI 10, PP 100); a clade containing *N. floridana*, *N. albigula*, *N. goldmani*, and *N. magister* (BP 100, DI 10, PP 100); and a clade containing *N. micropus* and *N. leucodon* (BP 100, DI 28, PP 100). Both MP and BI analyses join the latter two clades to the exclusion of the *N. mexicana* + *N. isthmica* + *N. picta* clade (BP 90, DI 9, PP 100). The only difference between MP and BI analyses is in the placement of *N. stephensi* within this clade. The MP analysis sets *N. stephensi* as sister to the three subclades (BP 57, DI 2) while the BI analyses place it at the base of the *N. mexicana* + *N. isthmica* + *N. picta* clade (PP 86–70).

The most major topological difference between the MP and BI analyses is the placement of *N. cinerea*. To further examine this difference, we constrained the MP searches to recover only those trees with *N. cinerea* allied with the *N. fuscipes* + *N. macrotis* + *N. lepida* clade. The 12 shortest trees generated by the constraint MP searches are 193 steps longer ($L = 4824$, CI = 0.40, RI = 0.65) than the unconstrained MP trees. A comparison of constrained and unconstrained MP topologies using a Templeton test suggests the MP and BI hypotheses are incompatible ($z = -10.4$, $P < 0.0001$). Conversely, BI searches forced to retain only those trees that place *N. cinerea* sister to all other woodrat species yield harmonic $-\ln L$ values (P_1: $-\ln L = 26151.1263$; P_2: $-\ln L = 26014.1294$; P_8: $-\ln L = 25889.2023$) significantly worse than the unconstrained BI topology according to a Mann–Whitney *U* test (P_1: $z = -48.7$, $P < 0.0001$; P_2: $z = -30.9$, $P < 0.0001$; P_8: $z = -32.6$, $P < 0.0001$). Finally, the 2ln Bayes factor

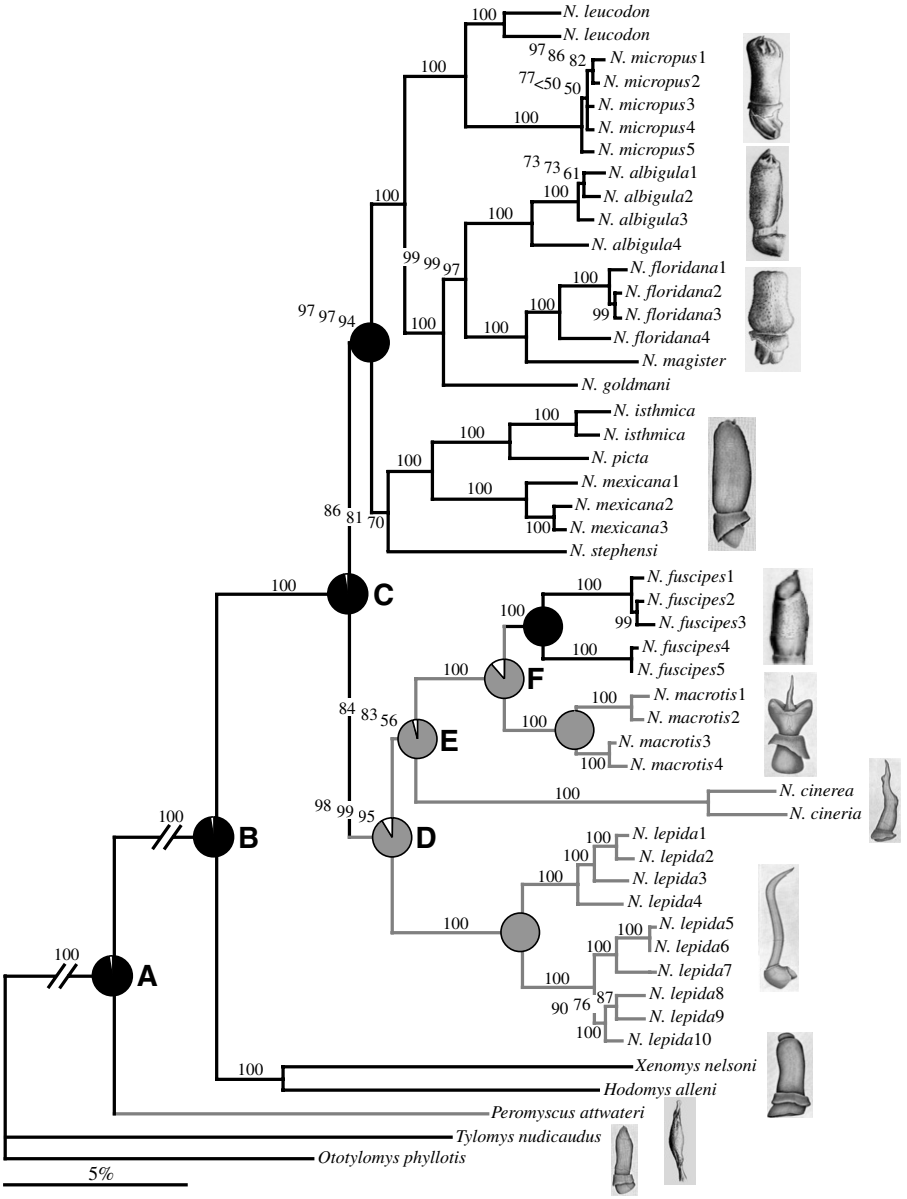

Fig. 4. Phylogenetic hypothesis of *Neotoma* relationships based on three separate BI analyses: one without data partitions (one model for all DNA; P_1), a second with two data partitions (a model for mtDNA and nucDNA; P_2), and a third with eight partitions (a model for each marker; P_8). Each BI analysis produced the same topology (P_1: harmonic mean $-\ln L = 26147.7036$; P_2: $-\ln L = 26011.3972$; P_8: $-\ln L = 25885.9923$). Numbers at nodes represent posterior probabilities (PP) for clades; a single number indicates an identical PP recovered for that node from all three analyses, while nodes with three values received different PP for P_1, P_2, and P_8 analyses, respectively. Branch lengths given from the P_8 analysis. Also shown is the ML reconstruction of phallus evolution in *Neotoma*. Lineages reconstructed with broad phalli illustrated with black lines, those with partially and completely narrow phalli with grey lines. Pie diagrams denote the proportion of reconstructions with broad (black), narrow (grey), and equivocal (white) states. Lettered nodes refer to discussion of character evolution in text. Illustrations by Karen Klitz, Q. R.S. and reproduced from Hooper (1960) with permission from the University of Michigan Museum of Zoology.

generally supports the BI phylogenetic hypothesis that places *N. cinerea* with the *N. fuscipes* + *N. macrotis* + *N. lepida* clade over the alternative MP arrangement (P_1: $2\ln B_{01} = 6.8453$; P_2: $2\ln B_{01} = 5.4645$; P_8: $2\ln B_{01} = 6.4200$).

3.3. Ancestral state reconstruction

Both MP and ML ancestral state reconstructions (ASR) on the three MP trees showed identical results, thus we simply show the MP reconstruction on the MP tree (Fig. 3). All nodes were 100% resolved as broad or narrow-formed phalli with the exception of 4 equivocal nodes: the base of *Neotoma* (excluding *Hodomys* and *Xenomys*; node A), the base of *Neotoma* excluding *N. cinerea* (node B), the base of the *N. fuscipes* + *N. macrotis* + *N. lepida* clade (node C), and the common ancestor of *N. fuscipes* and *N. macrotis* (node D).

Again, both MP and ML ASR on the 29,000 BI trees (P_8) yielded identical character distributions, thus we simply show the ML reconstruction on the BI topology (Fig. 4). While ancestral states are almost fully resolved on the BI phylog-

eny, six nodes could not be assigned to one state or the other with 100% certainty. Nodes A–C were present in all BI trees (29,000) and had high probabilities of being the broad state in MP ASR (each with 92% probability) and in ML ASR (all >99%) with no reconstructions resolving these nodes as narrow. Nodes D and E were only present in 27,964 and 15,155 BI trees, respectively. Nonetheless, node D was assigned the narrow state in 99% of the MP ASR and 94.5% of the ML ASR while node E was assigned the narrow state in 84% of MP ASR and 97.8% of ML ASR. Finally, node F was present in all BI trees and assigned the narrow state in 91% of the MP ASR and 91.4% of ML ASR.

4. Discussion

Elucidating the evolutionary processes underlying genital morphological diversity has the potential of providing tremendous insight into the generation and/or maintenance of species boundaries. The first step in understanding the evolution of genital diversity is to establish the phylogenetic context in which this diversity arose. By identifying the pattern of major character transitions throughout the evolutionary history of a group, we can begin to establish phylogenetically informed hypotheses concerning the processes leading to these patterns.

In this study, we use mitochondrial and nuclear loci whose rates of molecular evolution are, in combination, informative at the range of evolutionary depths that encompass the history of the genus *Neotoma*. We use these markers in conjunction with methods of phylogenetic estimation that allow the incorporation of minimally (MP and BI, P_1) to more highly parameterized (BI, P_2 and P_8) models of molecular evolution. Our estimate of phylogenetic relationships within *Neotoma* adds to the ongoing study of evolutionary affinities in this taxon. Furthermore, using our estimates of evolutionary relationships, we reconstruct the pattern of character transition in genital morphology that best explains the current distribution of morphotypes in extant taxa.

4.1. Molecular evolution

Molecular systematics has relied almost exclusively on sequence data from the mitochondrial genome for a wide variety of questions ranging from intraspecific phylogeographic structure (Avise, 2004) to evaluating deep phylogenetic relationships (e.g., Miya et al., 2001; Zardoya and Meyer, 2001). However, mtDNA data may not track organismal history if there has been selection on the mitochondria, introgression (Ballard and Whitlock, 2004) or high levels of homoplasy (Naylor and Brown, 1998). Thus, there is a strong emphasis in molecular systematics to discover additional markers from the nuclear genome that provide phylogenetic resolution at various evolutionary depths (Edwards et al., 2005).

In this study, we sequenced portions of four mitochondrial loci as well as fragments of four nuclear loci. The inclusion of additional data from the nuclear genome dramatically alters our understanding of woodrat phylogeny. Of particular importance for our study of character evolution, both MP and BI analyses conducted with mtDNA alone (not shown) place *N. cinerea* sister to the rest of *Neotoma*. However, combined BI analyses using both mtDNA and nucDNA suggest that *N. cinerea* is allied with *N. fuscipes*, *N. macrotis*, and *N. lepida*. In particular, FGB contains a substantial amount of variation and phylogenetic signal. Furthermore, indels in FGB provided an additional source of variation and such indels may be useful in other phylogenetic studies (Edwards et al., 2005). The nuclear FGB has been used in recent mammalian investigations (Seddon et al., 2001; Wickliffe et al., 2003; Krajewski et al., 2004; Spradling et al., 2004; Yu and Zhang, 2005) and also shows promise as a useful marker in non-avian reptiles (Creer et al., 2003; Chapple and Keogh, 2004). However, FGB has shown limited utility in resolving shallow avian relationships (Johnson and Clayton, 2000; Feldman and Omland, 2005), but appears suitable for resolving older bird divergences (Weibel and Moore, 2002; Prychitko and Moore, 2003; Moyle, 2004; Sheldon et al., 2005). In *Neotoma*, FGB is evolving at a slower rate than cyt *b*, yet more rapidly than 12S. Thus, FGB appears to be a promising nuclear marker for relatively shallow relationships at the intra-generic level in mammals.

4.2. Evolutionary relationships in the genus Neotoma

The taxonomic history of the genus *Neotoma* has been recently reviewed by Edwards and Bradley (2002). The genus traditionally includes formal subgeneric designations as well as several informal 'species groups' within these subgenera. Of the taxa studied here, *N. fuscipes* and *N. cinerea* were originally placed in their respective monotypic subgenera, *Homodontomys* and *Teonoma*, with the remaining taxa assigned to the subgenus *Neotoma* (Goldman, 1910). Species group names as applied by Edwards and Bradley (2002) are an attempt to reconcile previous applications of these group names (Goldman, 1910; Burt and Barkalow, 1942) with monophyletic, molecular-based clades. Inasmuch as these group names are useful in referring to particular monophyletic assemblages of species, we use them in our discussion of evolutionary relationships within the genus.

Like Edwards and Bradley (2002), we find good support for a clade uniting *N. leucodon* and *N. micropus* (their *micropus* group) as well as a clade consisting of *N. albigula, N. floridana*, *N. goldmani*, and *N. magister* (their *floridana* group). Both our MP and BI trees provide added support for the sister relationship between the two clades identified as the *micropus* and *floridana* groups. In contrast to Edwards and Bradley (2002), our BI analysis finds strong support for a sister relationship between the *micropus* + *floridana* groups and the *mexicana* group (*N. isthmica*, *N. mexicana*, and *N. picta*). The placement of *N. stephensi* remains somewhat ambiguous but both our parsimony and Bayesian analyses place *N. stephensi* quite strongly with the *micropus* + *floridana* + *mexicana* groups as opposed to the

clade containing *N. lepida* as suggested by Edwards and Bradley's (2002) likelihood topology (although no support values were estimated). *Neotoma stephensi* was originally considered to be a subspecies of *N. lepida* (Goldman, 1910), however, chromosomal evidence does not suggest a close relationship between these lineages (Mascarello and Hsu, 1976) and our study tentatively supports this view.

Goldman (1910) originally placed *N. fuscipes* in the monotypic subgenus *Homodontomys* while Burt and Barkalow (1942) suggested this species represented a unique species group within the subgenus *Neotoma*. Recent work has shown that what has traditionally been considered *N. fuscipes* represents a complex of at least two species (*N. fuscipes* and *N. macrotis*; Matocq, 2002a). Likewise, *N. lepida* represents a complex of two or more species (Mascarello, 1978; Patton and Álvarez-Castañeda, 2005). We find much added support for the sister relationship of the *N. fuscipes* and *N. lepida* complexes which Edwards and Bradley (2002) refer to as the *lepida* group.

Neotoma cinerea has been traditionally placed in the subgenus *Teonoma* (Goldman, 1910; Burt and Barkalow, 1942). Edwards and Bradley (2002) and our original parsimony analysis (see Section 4) fail to resolve the relationship of *N. cinerea* with other species and species groups within the genus. However, our Bayesian analyses strongly place *N. cinerea* in the clade containing the *N. fuscipes* and *N. lepida* complexes. A close relationship between *N. cinerea* and *N. fuscipes* is supported by Carleton's (1980) thorough morphological analysis, although this same analysis suggests that *N. lepida* is highly distinct from these and other species of the genus.

If original subgenus designations were to be applied to the molecular clades presented here, the subgenus *Neotoma* would represent a paraphyletic assemblage of the *floridana* + *micropus* + *mexicana* groups and the *N. lepida* complex. On the other hand, if original subgenus designations were to be applied to monophyletic lineages of relatively equal evolutionary depth within the genus, the recognition of *Homodontomys* (*N. fuscipes*) and *Teonoma* (*N. cinerea*) would require the establishment of several subgenus categories within *Neotoma*. Designation of formal intrageneric units will require further resolution of deep clade structure within the genus and the placement of *N. cinerea*, *N. stephensi* and other taxa not available for this study, especially *N. phenax* (subgenus *Teanopus*).

4.3. Evolution and development of morphological diversity in male genitalia

The genus *Neotoma* is part of the New World muroid subfamily Neotominae (Reig, 1980, 1984). Phallic diversity within New World muroids was originally categorized as 'complex' (four part baculum, presence of a terminal crater, mounds of soft tissue and other structures in the crater, and a complex vascular system) versus 'simple' morphotypes (single-bone baculum, usually no terminal crater, few or no mounds of soft tissue and other structures in the crater, and a rudimentary vascular system) (Hooper and Musser, 1964). *Neotoma* possesses the simple phallus type. Workers have argued that the simple phallus is the derived form in muroids (Hooper and Hart, 1962; Hooper and Musser, 1964). However, Carleton (1980) argued that a structural continuum exists between complex and simple morphotypes and that ancestral/derived relationships between these generalized forms are not evident. Carleton (1980) does suggest, however, that the narrow phallus form is derived relative to the broad form.

Our ancestral state reconstructions on the BI hypothesis of *Neotoma* phylogeny suggest that the ancestor of *Neotoma* had a broad phallus, that there was a single transition to the narrow form in the ancestor of the *N. cinerea* + *N. lepida* + *N. macrotis* + *N. fuscipes* clade, followed by a reversal to the broad form in *N. fuscipes* (Fig. 4). However, our ancestral state reconstructions on the MP estimate of *Neotoma* phylogeny are less resolved. Three equally parsimonious scenarios of phallus evolution emerge from this reconstruction, each requiring three steps (Fig. 3). First, if the ancestor of all *Neotoma* had a narrow phallus, there would have been one transition to the narrow form in the branch leading to this ancestor and two independent reversals to the broad form, once in *N. fuscipes*, and once in the clade uniting *N. leucodon* through *N. stephensi*. Second, all equivocal nodes could have had broad phalli requiring three independent transitions to the narrow form in *N. macrotis*, *N. lepida*, and *N. cinerea*. Third, the ancestor to all *Neotoma* could have had a broad phallus with a transition to the narrow form in *N. cinerea*, a separate narrowing in the ancestor of the *N. fuscipes* + *N. macrotis* + *N. lepida* clade, and a reversal to the broad form in *N. fuscipes*.

Differences in the MP and BI topologies lead to different scenarios of genital evolution in *Neotoma*. The primary difference between the MP and BI hypotheses is the placement of *N. cinerea*, yet constraint searches and subsequent topology tests suggest that the MP and BI hypotheses are each valid, but incompatible solutions. Thus, we explored the cause of the incongruence between the MP and BI methods of analysis. Because the conflict in MP and BI topologies involves *N. cinerea*, a long-branch taxon (Fig. 4), we suspected that either long-branch attraction (LBA; Felsenstein, 1978) or long-branch repulsion (LBR; Siddall, 1998) could be influencing our phylogenetic analyses. The problem of LBA can arise when parallel substitutions along long branches appear homologous but actually represent independent mutations. Thus, MP analyses can incorrectly group long branches as sister lineages (Felsenstein, 1978). Conversely, LBR can occur when models of molecular evolution overestimate homoplasy between sister taxa that possess long branches, forcing sister taxa apart (Siddall, 1998; but see Swofford et al., 2001).

To determine whether LBA influenced our MP estimate of *Neotoma* phylogeny, we employed the long-branch extraction test (Siddall and Whiting, 1999) by sequentially removing long-branch taxa, then conducting MP searches and assessing whether ingroup relationships changed. Because LBA is predominantly caused by outgroup taxa

(Bergsten, 2005), we removed outgroups, as well as *Hodomys* and *Xenomys*, to determine whether the position of *N. cinerea* would change. Likewise, we tested for LBR by performing the three Bayesian analyses after sequentially removing outgroup taxa as well as *Hodomys* and *Xenomys*. Indeed, upon removal of other long branches (outgroups, *Hodomys* and *Xenomys*) in the MP analysis, *N. cinerea* moved from a basal position to one sister to the *N. macrotis* + *N. fuscipes* clade as in the BI analyses. On the other hand, removal of outgroups, *Hodomys* and *Xenomys* in the BI analyses did not have any effect on ingroup topology. Thus, it appears that our original MP analysis was influenced by LBA (Siddall and Whiting, 1999). Furthermore, saturation plots (not shown) demonstrate that third position transitions and transversions are saturated in cyt *b*, and third position transitions are saturated in COII. The models of evolution implemented in ML-based BI searches are expected to mediate the effect of multiple hits on phylogenetic estimation (Swofford et al., 1996). Consequently, we favor the BI phylogenetic hypothesis. The BI topology suggests that, although extremely distinct from one another in phallic morphology (Hooper, 1960), *N. macrotis*, *N. cinerea*, and *N. lepida* are closely related and, therefore may share some underlying developmental processes that lead to a partially or completely narrow phallus (see below). Finally, given that *N. fuscipes* is nested within partially and completely narrow forms, the broad form has evolved independently at least once within *Neotoma*.

We can begin to suggest some simplistic developmental models for the range of phallic phenotypic diversity observed within *Neotoma* that we will test in future work. First, it is possible that the narrow form (either partial or complete) is the result of a single, major developmental change during ontogeny. One possible scenario is one wherein there is an important change early in development that has a drastic effect despite maintenance of the subsequent developmental sequence (Müller and Wagner, 1991). An early change of major effect has been proposed for the narrowing and elongation of the baculum in species of the rodent genus *Abrothrix* (Spotorno et al., 1990). A second scenario is one wherein the narrow morphotype is a late-stage lateral reduction of the broad form. In this scenario, the majority of the developmental processes generating a broad phallus would remain intact in narrow-form types with lateral reduction being generated by a late-stage developmental change. If either of these "single change of large effect" scenarios were the case, the reacquisition of the broad phallus in *N. fuscipes* would only require elimination of a single developmental alteration. That is, major components of the developmental process would remain unchanged between *N. fuscipes* and other broad-form taxa in the genus despite their distant evolutionary relationships.

On the other hand, generating a narrow phallus may require change throughout the developmental process and involve numerous components of the developmental mechanism. In this case, the phenotypic reversal seen in *N. fuscipes* would have arisen from a highly altered developmental background compared to other broad-form taxa. That is, although the adult phenotype of *N. fuscipes* is similar to other broad forms in the genus, the *N. fuscipes* morphology may be the result of a distinct set of developmental components.

Of course, the developmental processes that generate the phallus are themselves evolving, perhaps independently of their phenotypic endpoints (Wagner et al., 2000). As such, we may find extreme diversity in underlying developmental mechanisms making each of these lineages highly distinct despite apparent shared endpoint phenotypes. Nonetheless, we can gain a better understanding of the relationship between developmental processes and morphology by examining phallus development in select members of the genus *Neotoma* and other muroids that exhibit similar genital morphologies. Having detailed ontogenetic data for these forms will allow a more thorough comparative morphological analysis that captures the breadth of phenotypic variation beyond the initial, basic analysis of 'broad' vs. 'narrow' forms included here.

Several hypotheses have been put forth for the evolution of diversity in male genitalia including the 'lock and key' hypothesis, pleiotropism, and sexual selection (Eberhard, 1985; Edwards, 1993; Hosken and Stockley, 2004). However, understanding the rate and mode of evolution of genitalia will require knowledge of the underlying genetic architecture and development of copulatory organs (Nei et al., 1983; Wu and Palopoli, 1994). Understanding whether major morphological shifts in genitalia among species are the result of few genetic or developmental changes of large effect or numerous changes of small effect will provide significant insight into the potential tempo and mode of genital evolution and, potentially, the establishment and/or maintenance of species boundaries.

Acknowledgments

For kindly sharing tissues and specimens we thank R.D. Bradley (Texas Tech University), T.L. Yates, J.A. Cook and C. Parmenter (Museum of Southwestern Biology, University of New Mexico), J.L. Patton and C. Cicero (Museum of Vertebrate Zoology, University of California, Berkeley), P. Myers (Museum of Zoology, University of Michigan), D. Rogers (Monte L. Bean Museum, Brigham Young University), and M.D. Carleton and D.F. Schmidt (National Museum of Natural History, Smithsonian Institution). We thank J.L. Patton who generously provided unpublished cyt *b* sequences against which we could compare selected sequences generated in our lab and R.D. Bradley for helpful discussions concerning sequence discrepancies between our studies. We thank M.A. Thomas and L. Yang (Idaho State University Evolutionary Genomics Group) for computational assistance, E. O'Leary-Jepsen and M. Andrews of the Molecular Research Core Facility, and E.M. O'Neill and F.T. Burbrink for constructive phylogenetic discussions. For funding we thank an Idaho-NIH-BRIN (# P20 RR016454) for a seed grant to M.D. Matocq, and an Idaho-NIH-BRIN graduate fellowship to Q.R. Shurtliff and the American Society of Mammalogists.

Appendix A. Voucher specimens used and GenBank accession numbers for DNA sequence data

Taxon	General locality	Specimen No.; GenBank Nos.: 12S, 16S, COII, cyt *b*, MLR, MYH6, EN2, FGB
*Neotoma albigula*1	Yuma Co., Arizona	TK 77931; DQ179666, DQ179716, DQ179766, DQ179816*, DQ179866, DQ179916, DQ179966, DQ180016
*N. albigula*2	Chihuahua, Mexico	NK 17583; DQ179708, DQ179758, DQ179808, DQ179858*, DQ179908, DQ179958, DQ180008, DQ180058
*N. albigula*3	Apache Co., Arizona	NK 50148; DQ179707, DQ179757, DQ179807, DQ179857, DQ179907, DQ179957, DQ180007, DQ180057
*N. albigula*4	Otero Co., New Mexico	TK 74854; DQ179667, DQ179717, DQ179767, DQ179817, DQ179867, DQ179917, DQ179967, DQ180017
N. cinerea	Moffat Co., Colorado	NK 56291; DQ179705, DQ179755, DQ179805, DQ179855*, DQ179905, DQ179955, DQ180005, DQ180055
N. cinerea	Provo, Utah Co., Utah	BYU 17790; DQ179709, DQ179759, DQ179809, DQ179859, DQ179909, DQ179959, DQ180009, DQ180059
*N. floridana*1	Anderson Co., Texas	TK 52109; DQ179669, DQ179719, DQ179769, DQ179819, DQ179869, DQ179919, DQ179969, DQ180019
*N. floridana*2	Creek Co., Oklahoma	TK 27751; DQ179670, DQ179720, DQ179770, DQ179820*, DQ179870, DQ179920, DQ179970, DQ180020
*N. floridana*3	Lyon Co. Kansas	TK 28244; DQ179671, DQ179721, DQ179771, DQ179821*, DQ179871, DQ179921, DQ179971, DQ180021
*N. floridana*4	Richland Co., South Carolina	NK 64089; DQ179704, DQ179754, DQ179804, DQ179854*, DQ179904, DQ179954, DQ180004, DQ180054
*N. fuscipes*1	Colusa Co., California	MVZ 196405; DQ179672, DQ179722, DQ179772, DQ179822, DQ179872, DQ179922, DQ179972, DQ180022
*N. fuscipes*2	Siskiyou Co., California	MVZ 196386; DQ179673, DQ179723, DQ179773, DQ179823, DQ179873, DQ179923, DQ179973, DQ180023
*N. fuscipes*3	Modoc Co., California	MVZ 196394; DQ179674, DQ179724, DQ179774, DQ179824, DQ179874, DQ179924, DQ179974, DQ180024
*N. fuscipes*4	San Luis Obispo Co., California	MVZ 196371; DQ179675, DQ179725, DQ179775, DQ179825, DQ179875, DQ179925, DQ179975, DQ180025
*N. fuscipes*5	Contra Costa Co., California	MVZ 196356; DQ179676, DQ179726, DQ179776, DQ179826, DQ179876, DQ179926, DQ179976, DQ180026
N. goldmani	Nuevo Leon, Mexico	TK 28315; DQ179677, DQ179727, DQ179777, DQ179827*, DQ179877, DQ179927, DQ179977, DQ180027
N. isthmica	Chiapas, Mexico	TK 93296; DQ179679, DQ179729, DQ179779, DQ179829, DQ179879, DQ179929, DQ179979, DQ180029
N. isthmica	Oaxaca, Mexico	TK 93257; DQ179678, DQ179728, DQ179778, DQ179828*, DQ179878, DQ179928, DQ179978, DQ180028
*N. lepida*1	Orange Co., California	TK 77284; DQ179680, DQ179730, DQ179780, DQ179830, DQ179880, DQ179930, DQ179980, DQ180030
*N. lepida*2	San Diego Co., California	MVZ 197379; DQ179683, DQ179733, DQ179783, DQ179833, DQ179883, DQ179933, DQ179983, DQ180033
*N. lepida*3	San Benito Co., California	MVZ 195223; DQ179684, DQ179734, DQ179784, DQ179834, DQ179884, DQ179934, DQ179984, DQ180034
*N. lepida*4	Baja California, Mexico	MVZ 159790; DQ179685, DQ179735, DQ179785, DQ179835, DQ179885, DQ179935, DQ179985, DQ180035
*N. lepida*5	Mohave Co., Arizona	MVZ 197142; DQ179681, DQ179731, DQ179781, DQ179831, DQ179881, DQ179931, DQ179981, DQ180031
*N. lepida*6	Coconino Co., Arizona	NK 54420; DQ179703, DQ179753, DQ179803, DQ179853*, DQ179903, DQ179953, DQ180003, DQ180053
*N. lepida*7	Elko Co., Nevada	MVZ 197126; DQ179688, DQ179738, DQ179788, DQ179838, DQ179888, DQ179938, DQ179988, DQ180038
*N. lepida*8	Pima Co., Arizona	MVZ 202447; DQ179682, DQ179732, DQ179782, DQ179832, DQ179882, DQ179932, DQ179982, DQ180032
*N. lepida*9	Coconino Co., Arizona	MVZ 197094; DQ179686, DQ179736, DQ179786, DQ179836, DQ179886, DQ179936, DQ179986, DQ180036
*N. lepida*10	Yuma Co., Arizona	MVZ 197115; DQ179687, DQ179737, DQ179787, DQ179837, DQ179887, DQ179937, DQ179987, DQ180037
N. leucodon	Durango, Mexico	TK 48594; DQ179689, DQ179739, DQ179789, DQ179839*, DQ179889, DQ179939, DQ179989, DQ180039
N. leucodon	Kerr Co., Texas	TK 49716; DQ179665, DQ179715, DQ179765, DQ179815*, DQ179865, DQ179915, DQ179965, DQ180015
*N. macrotis*1	Placer Co., California	MDM 800; DQ179691, DQ179741, DQ179791, DQ179841, DQ179891, DQ179941, DQ179991, DQ180041
*N. macrotis*2	Fresno Co., California	MVZ 196585; DQ179692, DQ179742, DQ179792, DQ179842, DQ179892, DQ179942, DQ179992, DQ180042
*N. macrotis*3	Orange Co., California	TK 77285; DQ179693, DQ179743, DQ179793, DQ179843*, DQ179893, DQ179943, DQ179993, DQ180043
*N. macrotis*4	Riverside Co., California	TK 83707; DQ179694, DQ179744, DQ179794, DQ179844*, DQ179894, DQ179944, DQ179994, DQ180044

N. magister	Madison Co., Virginia	NK 64158; DQ179706, DQ179756, DQ179806, DQ179856*, DQ179906, DQ179956, DQ180006, DQ180056
*N. mexicana*1	Michoacan, Mexico	TK 45631; DQ179695, DQ179745, DQ179795, DQ179845, DQ179895, DQ179945, DQ179995, DQ180045
*N. mexicana*2	Las Animas Co., Colorado	TK 51346; DQ179696, DQ179746, DQ179796, DQ179846*, DQ179896, DQ179946, DQ179996, DQ180046
*N. mexicana*3	Los Alamos Co., New Mexico	TK 78350; DQ179697, DQ179747, DQ179797, DQ179847, DQ179897, DQ179947, DQ179997, DQ180047
*N. micropus*1	Floyd Co., Texas	TK 54559; DQ179668, DQ179718, DQ179768, DQ179818, DQ179868, DQ179918, DQ179968, DQ180018
*N. micropus*2	Roosevelt Co., New Mexico	TK 31643; DQ179698, DQ179748, DQ179798, DQ179848*, DQ179898, DQ179948, DQ179998, DQ180048
*N. micropus*3	Dimmitt Co., Texas	TK 84557; DQ179690, DQ179740, DQ179790, DQ179840*, DQ179890, DQ179940, DQ179990, DQ180040
*N. micropus*4	Dimmitt Co., Texas	TK 84556; DQ179700, DQ179750, DQ179800, DQ179850*, DQ179900, DQ179950, DQ180000, DQ180050
*N. micropus*5	Otero Co., New Mexico	TK 77270; DQ179699, DQ179749, DQ179799, DQ179849, DQ179899, DQ179949, DQ179999, DQ180049
N. picta	Guerrero, Mexico	TK 93390; DQ179701, DQ179751, DQ179801, DQ179851, DQ179901, DQ179951, DQ180001, DQ180051
N. stephensi	Navaho Co., Arizona	TK 77928; DQ179702, DQ179752, DQ179802, DQ179852*, DQ179902, DQ179952, DQ180002, DQ180052
Hodomys alleni	Michoacan, Mexico	TK 45042; DQ179660, DQ179710, DQ179760, DQ179810*, DQ179860, DQ179910, DQ179960, DQ180010
Xenomys nelsoni	Jalisco, Mexico	TK 19559; DQ179663, DQ179713, DQ179763, DQ179813*, DQ179863, DQ179913, DQ179963, DQ180013
Peromyscus attwateri	McIntosh Co., Oklahoma	TK 23396; DQ179661, DQ179711, DQ179761, DQ179811, DQ179861, DQ179911, DQ179961, DQ180011
Tylomys nudicaudus	Izabal, Guatemala	TK 41551; DQ179662, DQ179712, DQ179762, DQ179812*, DQ179862, DQ179912, DQ179962, DQ180012
Ototylomys phyllotis	Atlantida, Honduras	TK 101714; DQ179664, DQ179714, DQ179764, DQ179814, DQ179864, DQ179914, DQ179964, DQ180014

Abbreviations are: NK, Museum of Southwestern Biology, University of New Mexico; MVZ, Museum of Vertebrate Zoology, University of California, Berkeley; TK, Museum of Texas Tech University; BYU, Monte L. Bean Museum, Brigham Young University; MDM, field collection number of Marjorie D. Matocq; DQ, GenBank (http://www.ncbi.nlm.nih.gov). Numbers in taxon column correspond to position of specimen in Figs. 2 and 3. Cyt *b* sequences that differ between this study and Edwards and Bradley (2002) despite using the same source material are indicated with an asterisk.

Appendix B. Reference material for phallus morphology for ancestral state reconstructions

Taxon	Specimen No. Literature source
Neotoma albigula	MVZ 200703, UMMZ 83665, UMMZ 110447
N. cinerea	Hooper (1960), UMMZ 110202
N. floridana	UMMZ 110378, UMMZ 115698
N. fuscipes	Matocq (2002a)
N. isthmica	Hooper (1960), UMMZ 109668, UMMZ 112230, UMMZ 112227, UMMZ 118231
N. lepida	Hooper (1960)
N. leucodon	UMMZ 100704, UMMZ 100707, UMMZ 100710
N. macrotis	Hooper (1960); Matocq (2002a)
N. magister	USNM 283065
N. mexicana	UMMZ 100702
N. micropus	UMMZ 99175, UMMZ 99176, UMMZ 109721
N. picta	UMMZ 109666, UMMZ 109667
N. stephensi	Hooper (1960)
Hodomys alleni	Hooper (1960)
Xenomys nelsoni	Hooper (1960)
Peromyscus attwateri	MSB 73860, MSB 73861
Tylomys nudicaudus	USNM 583238
Ototylomys phyllotis	Hooper (1960)

Abbreviations used: MSB, Museum of Southwestern Biology, University of New Mexico; UMMZ, Museum of Zoology, University of Michigan; USNM, National Museum of Natural History, Smithsonian Institution. Specimens illustrated for this study and included in Figs. 3 and 4 are underlined.

References

Adkins, R.M., Honeycutt, R.L., 1994. Evolution of the primate cytochrome *c* oxidase subunit II gene. J. Mol. Evol. 38, 215–231.

Adler, N.T., 1969. Effects of the male's copulatory behavior on successful pregnancy of the female rat. J. Comp. Physiol. Psychol. 69, 613–622.

Akaike, H., 1974. A new look at the statistical model identification. IEEE Trans. Autom. Control 19, 716–723.

Altschul, S.F., Madden, T.L., Schäffer, A.A., Zhang, J., Zhang, Z., Miller, W., Lipman, D.J., 1997. Gapped BLAST and PSI-BLAST: a new generation of protein database search programs. Nucleic Acids Res. 25, 3389–3402.

Arnqvist, G., 1997. The evolution of animal genitalia: distinguishing between hypotheses by single species studies. Biol. J. Linn. Soc. 60, 365–379.

Avise, J.C., 2004. Molecular Markers, Natural History, and Evolution, 2nd ed. Sinauer Associates, Inc., Sunderland, MA.

Bradley, R.D., Baker, R.J., 2001. A test of the genetic species concept: cytochrome-*b* sequences and mammals. J. Mamm. 82, 960–973.

Bradley, R.D., Schmidly, D.J., 1987. The glans penes and bacula in Latin American taxa of the *Peromyscus boylii* group. J. Mamm. 68, 595–616.

Ballard, J.W.O., Whitlock, M.C., 2004. The incomplete natural history of mitochondria. Molec. Ecol. 13, 729–744.

Bergsten, J., 2005. A review of long-branch attraction. Cladistics 21, 163–193.

Brandley, M.C., Schmitz, A.C., Reeder, T.W., 2005. Partitioned Bayesian analyses, partition choice, and the phylogenetic relationships of scincid lizards. Syst. Biol. 54, 373–390.

Bremer, K., 1994. Branch support and tree stability. Cladistics 10, 295–304.

Burt, W.H., Barkalow, F.S., 1942. A comparative study of the bacula of wood rats (subfamily Neotominae). J. Mamm. 23, 287–297.

Carleton, M.D., 1980. Phylogenetic relationships in neotomine-peromyscine rodents (Muriodea) and a reappraisal of the dichotomy within New World Cricetinae. Misc. Publ. Zool. Univ. Mich. 157, 1–146.

Chapple, D.G., Keogh, J.S., 2004. Parallel adaptive radiations in arid and temperate Australia: molecular phylogeography and systematics of the *Egernia whitii* (Lacertilia: Scincidae) species group. Biol. J. Linn Soc. 83, 157–173.

Creer, S., Malhotra, A., Thorpe, R.S., 2003. Assessing the phylogenetic utility of four mitochondrial genes and a nuclear intron in the Asian pit viper genus, *Trimeresurus*: separate, simultaneous and conditional data combination analyses. Mol. Biol. Evol. 20, 1240–1251.

Dewsbury, D.A., 1975. Diversity and adaptation in rodent copulatory behavior. Science 190, 947–954.

Eberhard, W.G., 1985. Sexual Selection and Animal Genitalia. Harvard University Press, Cambridge, MA.

Edwards, R., 1993. Entomological and mammalogical perspectives on genital differentiation. Trends Ecol. Evol. 8, 406–409.

Edwards, C.W., Bradley, R.D., 2002. Molecular systematics of the genus *Neotoma*. Mol. Phylogenet. Evol. 25, 489–500.

Edwards, S.V., Jennings, W.B., Shedlock, A.M., 2005. Phylogenetics of modern birds in the era of genomics. Proc. R. Soc. Biol. Sci. Ser. B 272, 979–992.

Farris, J.S., 1983. The logical basis of phylogenetic analysis. In: Platnick, N., Funk, V.A. (Eds.), Advances in Cladistics. Columbia University Press, New York, NY, pp. 7–36.

Feldman, C.R., Omland, K.E., 2005. Phylogenetics of the common raven complex (*Corvus*: Corvidae) and the utility of ND4, COI, and intron seven of the nuclear gene β-fibrinogen in avian molecular systematics. Zool. Scr. 34, 145–156.

Felsenstein, J., 1978. Cases in which parsimony or compatibility methods will be positively misleading. Syst. Zool. 27, 401–410.

Felsenstein, J., 1985. Confidence limits on phylogenies: an approach using the bootstrap. Evolution 39, 783–791.

Goldman, E.A., 1910. Revision of the woodrats of the genus *Neotoma*. North Am. Fauna 31, 1–124.

Grafen, A., Hails, R., 2004. Modern statistics for the life sciences. Oxford University, Oxford.

Hershkovitz, P., 1979. Living new world monkeys (Platyrrhini) with an introduction to primates. vol. 1. University of Chicago Press, Chicago IL.

Hibbett, D.S., Donoghue, M.J., 2001. Analysis of character correlations among wood decay mechanisms, mating systems, and substrate ranges in homobasidiomycetes. Syst. Biol. 50, 215–242.

Hooper, E.T., 1958. The male phallus in mice of the genus *Peromyscus*. Misc. Publ. Mus. Zool. Univ. Mich. 105, 1–24.

Hooper, E.T., 1960. The glans penis in *Neotoma* (Rodentia) and allied genera. Occas. Pap. Mus. Zool. Univ. Mich. 613, 1–10.

Hooper, E.T., Hart, B.S., 1962. A synopsis of recent North American microtine rodents. Misc. Publ. Mus. Zool. Univ. Mich. 123, 1–68.

Hooper, E.T., Musser, G.G., 1964. The glans penis in Neotropical cricetines (Family Muridae) with comments on classification of muroid rodents. Misc. Publ. Mus. Zool. Univ. Mich. 123, 1–57.

Hosken, D.J., Stockley, P., 2004. Sexual selection and genital evolution. Trends Ecol. Evol. 19, 87–93.

Huelsenbeck, J.P., Ronquist, F., 2001. MrBayes: Bayesian inference of phylogenetic trees. Bioinformatics 17, 754–755.

Irwin, D.M., Kocher, T.D., Wilson, A.C., 1991. Evolution of the cytochrome b gene of mammals. J. Mol. Evol. 32, 82–102.
Johnson, K.P., Clayton, D.H., 2000. A molecular phylogeny of the dove genus *Zenaida*. Condor 102, 864–870.
Kass, R.E., Raftery, A.E., 1995. Bayes factors. J. Am. Stat. Assoc. 90, 773–795.
Krajewski, C., Moyer, G.R., Sipiorski, J.T., Fain, M.G., Westerman, M., 2004. Molecular systematics of the enigmatic 'phascolosoricine' marsupials of New Guinea. Aust. J. Zool. 52, 389–415.
Krutzch, P.H., Vaughn, T.A., 1955. Additional data on the bacula of North American bats. J. Mamm. 36, 96–100.
Larget, B., Simon, D.L., 1999. Markov chain Monte Carlo algorithms for the Bayesian analysis of phylogenetic trees. Mol. Biol. Evol. 16, 750–759.
Lessa, E.P., Cook, J.A., Patton, J.L., 2003. Genetic footprints of demographic expansion in North America, but not Amazonia, during the Late Quaternary. Proc. Natl. Acad. Sci. USA 100, 10331–10334.
Lewis, P.O., 2001. A likelihood approach to estimating phylogeny from discrete morphological character data. Syst. Biol. 50, 913–925.
Lidicker, W.Z., 1968. A phylogeny of New Guinea rodent genera based on phallic morphology. J. Mamm. 49, 609–643.
Lidicker, W.Z., Brylski, P.V., 1987. The conilurine rodent radiation of Australia, analyzed on the basis of phallic morphology. J. Mamm. 68, 617–641.
Long, C.A., Frank, T., 1968. Morphometric variation and function in the baculum, with comments on correlation of parts. J. Mamm. 49, 32–43.
Lutzoni, F., Pagel, M., Reeb, V., 2001. Major fungal lineages are derived from lichen symbiotic ancestors. Nature 411, 937–940.
Lyons, L.A., Laughlin, T.F., Copeland, N.G., Jenkins, N.A., Womack, J.E., O'Brien, S.J., 1997. Comparative anchor tagged sequences (CATS) for integrative mapping of mammalian genomes. Nat. Genet. 15, 47–56.
Maddison, D.R., Maddison, W.P., 2005. MacClade 4: Analysis of phylogeny and character evolution. Version 4.08. Sinauer Associates, Sunderland, MA.
Maddison, W.P., Maddison, D.R., 2004. Mesquite: a modular system for evolutionary analysis. Version 1.05. Available from: http://mesquiteproject.org.
Martin, C.O., Schmidly, D.J., 1982. Taxonomic review of the pallid bat *Antrozous pallidus* (LeConte). Spec. Publ. Mus. Texas Tech Univ. 18, 1–48.
Mascarello, J.T., 1978. Chromosomal, biochemical, mensural, penile, and cranial variation in desert woodrats (*Neotoma lepida*). J. Mamm. 59, 477–495.
Mascarello, J.T., Hsu, T.C., 1976. Chromosome evolution in woodrats, genus *Neotoma* (Rodentia: Cricetidae). Evolution 30, 152–169.
Matocq, M.D., 2002a. Morphological and molecular analysis of a contact zone in the *Neotoma fuscipes* species complex. J. Mamm. 83, 866–883.
Matocq, M.D., 2002b. Phylogeographical and regional history of the dusky-footed woodrat, *Neotoma fuscipes*. Mol. Ecol. 11, 229–242.
Matthews, M., Adler, N.T., 1977. Facultative and inhibitory influences of reproductive behavior on sperm transport in rats. J. Comp. Physiol. Psych. 91, 727–742.
Miya, M., Kawaguchi, A., Nishida, M., 2001. Mitogenomic exploration of higher teleostean phylogenies: a case study for moderate-scale evolutionary genomics with 38 newly determined complete mitochondrial DNA sequences. Mol. Biol. Evol. 18, 1993–2009.
Moyle, R.G., 2004. Phylogenetics of barbets (Aves: Piciformes) based on nuclear and mitochondrial DNA sequence data. Mol. Phylogenet. Evol. 30, 187–200.
Müller, G.B., Wagner, G.P., 1991. Novelty in evolution: restructuring the concept. Annu. Rev. Ecol. Syst. 22, 229–256.
Naylor, G.J.P., Brown, W.M., 1998. *Amphioxus* mitochondrial DNA, chordate phylogeny, and the limits of inference based on comparisons of sequences. Syst. Biol. 47, 61–76.
Nei, M., Maruyama, T., Wu, C.I., 1983. Models of evolution of reproductive isolation. Genetics 103, 557–579.
Nylander, J.A.A., 2004. MrModeltest 2.1. Program distributed by the author. Evolutionary Biology Centre, Uppsala University, Sweden.
Nylander, J.A.A., Ronquist, F., Huelsenbeck, J.P., Nieves-Aldrey, J.L., 2004. Bayesian phylogenetic analysis of combined data. Syst. Biol. 53, 47–67.
Pagel, M., 1999. Inferring the historical patterns of biological evolution. Nature 401, 877–884.
Patterson, B.D., Thaeler Jr., C.S., 1982. The mammalian baculum: hypotheses on the nature of bacular variability. J. Mamm. 63, 1–15.
Patton, J.L., Alvarez-Castañeda, S.T., 2005. Phylogeography of the desert woodrat, *Neotoma lepida*, with comments on systematics and biogeographic history.
Posada, D., Buckley, T.R., 2004. Model selection and model averaging in phylogenetics: advantages of AIC and Bayesian approaches over likelihood ratio tests. Syst. Biol. 53, 793–808.
Prasad, M., 1974. Mannliche Geschlechtsorgane. Hanbuch der Zoologie. 8 Band/51Lieferung 9, pp. 1–15.
Prychitko, T.M., Moore, W.S., 2003. Alignment and phylogenetic analysis of β-Fibrinogen intron 7 sequences among avian orders reveal conserved regions within the intron. Mol. Biol. Evol. 20, 762–771.
Rannala, B., Yang, Z.H., 1996. Probability distribution of molecular evolutionary trees: a new method of phylogenetic inference. J. Mol. Evol. 43, 304–311.
Reeder, S.A., Bradley, R.D., 2004. Molecular systematics of neotomine-peromyscine rodents based on the dentin matrix protein 1 gene. J. Mamm. 85, 1194–1200.
Reig, O.A., 1980. A new fossil genus of South American cricetid rodents allied to *Wiedomys*, with an assessment of the Sigmodontinae. J. Zool. 192, 257–281.
Reig, O.A., 1984. Distribuição geográfica e história evolutiva dos roedores muroides sulamericanos (Cricetidae: Sigmodontinae). Rev. Bras. Genét. 7, 333–365.
Ronquist, F., Huelsenbeck, J.P., 2003. MRBAYES 3: Bayesian phylogenetic inference under mixed models. Bioinformatics 19, 1572–1574.
Saiki, R.K., Gelfand, D.H., Stoffel, S., Scharf, S.J., Higuchi, R.G., Horn, T.T., Mullis, K.B., Erlich, H.A., 1988. Primer directed enzymatic amplification of DNA with a thermostable DNA polymerase. Science 239, 487–491.
Sanchez-Gracia, A., Aguade, M., Rozas, J., 2003. Patterns of nucleotide polymorphism and divergence in the odorant-binding protein genes OS-E and OS-F: Analysis in the *melanogaster* species subgroup of *Drosophila*. Genetics 165, 1279–1288.
Sanger, F., Nicklen, S., Coulson, A.R., 1977. DNA sequencing with chain-terminating inhibitors. Proc. Natl. Acad. Sci. USA 74, 5463–5467.
Schluter, D., Price, T., Mooers, A.O., Ludwig, D., 1997. Likelihood of ancestor states in adaptive radiation. Evolution 51, 1699–1711.
Seddon, J.M., Santucci, F., Reeve, N.J., Hewitt, G.M., 2001. DNA footprints of European hedgehogs, *Erinaceus europaeus* and *E. concolor*: Pleistocene refugia, postglacial expansion and colonization routes. Mol. Ecol. 10, 2187–2198.
Sheldon, F.H., Whittingham, L.A., Moyle, R.G., Slikas, B., Winkler, D.W., 2005. Phylogeny of swallows (Aves: Hirundinidae) estimated from nuclear and mitochondrial DNA sequences. Mol. Phylogenet. Evol. 35, 254–270.
Short, R.V., 1979. Sexual selection and its component parts, somatic and genital selection, as illustrated by man and the great apes. Adv. Study Behav. 9, 131–158.
Siddall, M.E., 1998. Success of parsimony in the four-taxon case: long-branch repulsion by likelihood in the Farris Zone. Cladistics 14, 209–220.
Siddall, M.E., Whiting, M.F., 1999. Long-branch abstractions. Cladistics 15, 9–24.
Smith, M.F., Patton, J.L., 1993. Diversification of South American muroid rodents: evidence from mitochondrial DNA sequence data for the Akodontine tribe. Biol. J. Linn. Soc. 50, 149–177.
Sokal, R.R., Rohlf, F.J., 1995. Biometry, the Principles and Practice of Statistics in Biological Research, 3rd ed. W.H. Freeman and Company, New York, NY.
Sorenson, M.D., 1999. TreeRot. Boston University, Boston, MA.
Spotorno, A.E., Zuleta, C.A., Cortes, A., 1990. Evolutionary systematics and heterochrony in *Abrothrix* species (Rodentia, Cricetinae). Evolución Biologica 4, 37–62.

Spradling, T.A., Brant, S.V., Hafner, M.S., Dickerson, C.J., 2004. DNA data support a rapid radiation of pocket gopher genera (Rodentia: Geomyidae). J. Mamm. Evol. 11, 105–125.

Sullivan, R.M., Calhoun, S.W., Greenbaum, I.F., 1990. Geographic variation in genital morphology among insular and mainland populations of *Peromyscus maniculatus* and *Peromyscus oreas*. J. Mamm. 71, 48–58.

Swofford, D.L., 2002. PAUP*: Phylogenetic analysis using parsimony (*and other methods). Sinauer Associates Inc., Sunderland, MA.

Swofford, D.L., Olson, G.J., Waddell, P.J., Hillis, D.M., 1996. Phylogenetic inference. In: Hillis, D.M., Moritz, C., Mable, B.K. (Eds.), Molecular Systematics. Sinauer Associates Inc., Sunderland, MA, pp. 407–514.

Swofford, D.L., Waddell, P.J., Huelsenbeck, J.P., Foster, P.G., Lewis, P.O., Rogers, J.S., 2001. Bias in phylogenetic estimation and its relevance to the choice between parsimony and likelihood methods. Syst. Biol. 50, 525–539.

Templeton, A.R., 1983. Phylogenetic inference from restriction endonuclease cleavage site maps with particular reference to the evolution of humans and the apes. Evolution 37, 221–244.

Vacquier, V.D., Swanson, W.J., Lee, Y.H., 1997. Positive Darwinian selections on two homologous fertilization proteins: what is the selective pressure driving their divergence? J. Mol. Evol. 44, S15–S22.

Wagner, G.P., Chiu, C.H., Laubichler, M., 2000. Developmental evolution as a mechanistic science: the inference from developmental mechanisms to evolutionary processes. Am. Zool. 40, 819–831.

Watts, R.A., Palmer, C.A., Feldhoff, R.C., Feldhoff, P.W., Houck, L.D., Jones, A.G., Pfrender, M.E., Rollmann, S.M., Arnold, S.J., 2004. Stabilizing selection on behavior and morphology masks positive selection on the signal in a salamander pheromone signaling complex. Mol. Biol. Evol. 21, 1032–1041.

Weibel, A.C., Moore, W.S., 2002. A test of mitochondrial gene-based phylogeny of woodpeckers (genus *Picoides*) using an independent nuclear gene, β-fibrinogen intron 7. Mol. Phylogenet. Evol. 22, 247–257.

Wickliffe, J.W., Hoffmann, F.G., Carroll, D.S., Dunina-Barkovskaya, Y.V., Bradley, R.D., Baker, R.J., 2003. Intron 7 (FGB-I7) of the fibrinogen B beta polypeptide (FGB): a nuclear DNA phylogenetic marker for mammals. Occas. Pap. Mus. Texas Tech Univ. 219, 1–6.

Wyckoff, G.J., Wang, W., Wu, C.I., 2000. Rapid evolution of male reproductive genes in the descent of man. Nature 403, 304–309.

Wu, C.I., Palopoli, M.F., 1994. Genetics of postmating reproductive isolation in animals. Annu. Rev. Genet. 28, 283–308.

Yang, Z., 1996. Maximum likelihood models for combined analyses of multiple sequence data. J. Mol. Evol. 42, 587–596.

Yu, L., Zhang, Y.P., 2005. Phylogenetic studies of pantherine cats (Felidae) based on multiple genes, with novel application of nuclear beta-fibrinogen intron 7 to carnivores. Mol. Phylogenet. Evol. 35, 483–495.

Zardoya, R., Meyer, A., 2001. On the origin of and phylogenetic relationships among living amphibians. Proc. Natl. Acad. Sci. USA 98, 7380–7383.